14th International Particle Accelerator Conference,Venice, Italy JACoW Publishing
ISBN: 978-3-95450-231-8 ISSN: 2673-5490 doi: 10.18429/JACoW-IPAC2023-MOPA091

THE STATUS OF THE INTERACTION REGION DESIGN AND MACHINE DETECTOR INTERFACE OF THE FCC-ee *

M. Boscolo[†1], A. Ciarma[1], F. Fransesini[1], S. Lauciani[1], F. Bosi[2], F. Palla[2], A. Novokhatski[3], T. Raubenheimer[3], M. K.Sullivan[3], A. Abramov[4], K. D. J. André[4], J. Bauche[4], M. Benedikt[4], G. Broggi[1,4,5], H. Burkhardt[4], J.C. Eriksson[4], A.P. Foussat[4], R. Kersevan[4], M. Koratzinos[4], A. Lechner[4], K. Oide[4], J. Salvesen[4,6], L. Watrelot[4], M. Wendt[4], F. Zimmermann[4], M. Dam[7], B. Parker[8], P.N. Burrows[6], L. Brunetti[9], S. Grabon[9], E. Montbarbon[9], F. Poirier[9]
[1] INFN-LNF, Frascati, Italy, [2] INFN-Pisa, Italy, [3] SLAC, CA, USA
[4] CERN, Geneva, Switzerland, [5] Sapienza U., Rome, Italy, [6] JAI, Oxford, UK
[7] NBI, Copenhagen, Denmark, [8] BNL, NY, USA, [9] LAPP, Annecy, France

Abstract

We present the latest development for the FCC-ee interaction region. It represents a major challenge for the FCC-ee collider, which has to achieve extremely high luminosity over a wide range of centre-of-mass energies. The FCC-ee will host two or four high-precision experiments. The machine parameters have to be well controlled and the design of the machine-detector-interface has to be carefully optimized. In particular, the complex final focus hosted in the detector region has to be carefully designed, and the impact of beam losses and of any type of radiation generated in the interaction region, including beamstrahlung, have to be simulated in detail. We discuss mitigation measures and the expected impact of beam losses and radiation on the detector background. We also report on the progress of the mechanical model of the interaction region layout, including the engineering design of the central beam pipe, and other MDI components.

INTRODUCTION

FCC-ee is a high luminosity and high energy circular electron-positron collider with an optimised circumference of almost 91 km, to be built in the Lake Geneva basin. Its physics goals are to carry out precision studies and searches for rare decays in the centre-of-mass energy range from 90 to 365 GeV [1]. The optics and layout are designed such that the interaction points (IPs) and arcs overlap with those of a successive energy-frontier hadron collider FCC-hh [2]. The Machine Detector Interface (MDI) challenges vary with the operating energy. On the Z-pole, the FCC-ee will be operating in a high-beam current and high-luminosity mode. By contrast, when running at the $t\bar{t}$ threshold the FCC-ee will face the highest photon energies from synchrotron radiation (SR), albeit at much lower beam current. The most relevant parameters for the interaction region (IR) design of FCC-ee are listed in Table 1. The general collider layout is shown in Fig. 1.

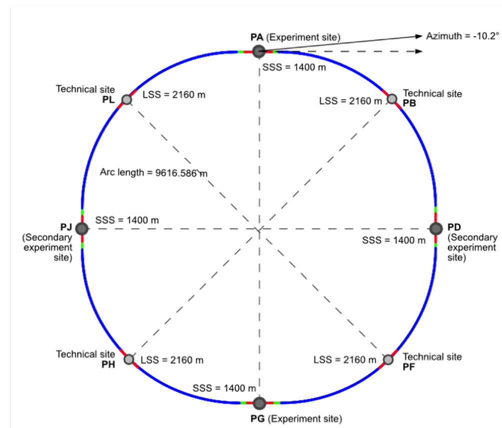

Figure 1: FCC-ee layout with four IPs, where PA, PG, PD, and PJ indicate the experiment sites; PF is the collimation section, PB the injection/extraction section; and PH and PL host the radio-frequency systems.

IR DESIGN

The IR design must accommodate all operation points. The IP β-functions are optimised for each running energy [3], taking into account various constraints. The crab-waist collision scheme [4, 5] associated with a large Piwinski angle and a low β_y is chosen for the FCC-ee design. This scheme reduces the hourglass effect, and allows the β_y at the interaction point (IP) to be smaller than the bunch length. This scheme requires a small horizontal beam size and a large crossing angle at the IP, set to 30 mrad allowing the beams to enter/exit with separate beam pipes at about 1.2 m after the IP. So, the initial final focus defocusing quadrupole (QC1) can be a separate magnet for each beam, with about 6 cm of space between the beams at the face of QC1 (2.2 m). An asymmetric optics minimises the emission of SR fans onto the IR by a weaker bending of the incoming beam trajectory. The asymmetric bending also generates the 30 mrad horizontal crossing angle. Stronger dipoles after the collision point help bring the outgoing beam back to the vicinity of the counterpropagating incoming beam. Both beams not only share a common tunnel but also share twin-aperture dipole magnets in the collider arcs. A wider tunnel in the range ±1.2 km around the IP provides space for this layout.

* This work was partially supported by the EC HORIZON 2020 project FCC-IS, grant agreement No. 951754.
† manuela.boscolo@lnf.infn.it

ISBN: 978-3-95450-231-8 ISSN: 2673-5490 doi: 10.18429/JACoW-IPAC2023-MOPA091

Outside the IR, the FCC-ee, the booster as well as the subsequent collider, FCC-hh, will all be housed in the same tunnel that has an inner diameter of 5.5 m. The booster has to bypass the FCC-ee detector at the IP with a transverse offset of at least 8 m. In addition to the SC Final Focus Quadrupoles (FFQ), the IR magnet system comprises a compensating solenoid spanning a distance 1.25 to 2.2 m from the IP on either side and by screening solenoids surrounding the final quadrupole magnets, which shield the latter against the 2 T detector magnetic field. The compensating solenoid in front of the FFQ has approximately twice the detector field strength, but with opposite sign, so as to cancel the total integral of the detector field between the final-focus magnets, which locally corrects the betatron coupling and avoids any net spin rotation. The detector magnetic field is set to 2 T in order to keep the blow-up due to the residual dispersion and synchrotron radiation in the solenoid fringe fields at an acceptable level, namely at a fraction of the nominal ~1 pm vertical emittance. Just in front of the compensating solenoids sits a luminosity calorimeter (lumical), which is designed to measure the luminosity to an absolute precision of 10^{-4} [6]. Two crab sextupoles, placed at a proper phase advance with respect to the IP, rotate the β_y function at the IR so that its waist is on the central trajectory of the opposite colliding beam and, in addition, they suppress betatron and synchro-betatron resonances introduced by the large Piwinski angle. The crab sextupoles for the FCC-ee will also be part of the vertical chromatic correction system. They are located asymmetrically with respect to the IP, at about 745 m before and 276 m after the IP. The vertical chromaticity correction sextupoles ate located at 497 m before and 118 m after the IP. These magnets are all be superconducting. Before further advancing with the magnet design, the multipole error tolerances and maximum integrated field strength need to be confirmed. The FFQ IR magnets are based on the mature canted coil technology recently developed and produced in series on the CERN HL-LHC project [8]. Furthermore, a combined direct wind of IR correction coils have been proposed [9]. Special beam position monitors (BPM) are required to be placed near the lumical as well as next to the SC FFQ and attached to the warm beam pipe. The former are supported independently from these magnets. The small space available in this area sets strict constraints on the BPM design.

Table 1: Preliminary Key Parameters of FCC-ee as Evolved from the CDR Parameters, for Scenarios with 4 IPs [7]. (*) Lifetime is by radiative Bhabhas and beamstrahlung.

Running mode	Z	W	ZH	$t\bar{t}$
Circumference [km]	90.659			
Beam energy [GeV]	45.6	80	120	182.5
Bunches/beam	15880	880	248	40
Beam current [mA]	1270	135	26.7	5.0
Lum. / IP [10^{34}cm^{-2}s^{-1}]	140	19.4	7.26	1.25
SR power / ring [MW]	50			
σ_z (SR) [mm]	5.60	3.55	3.34	1.94
σ_z (BS) [mm]	12.7	8.01	6.00	2.74
En. Spread σ_δ (SR) [%]	0.039	0.069	0.103	0.157
En. Spread σ_δ (BS) [%]	0.089	0.154	0.185	0.221
Rms hor. emit. ε_x [nm]	0.71	2.16	0.64	1.469
Rms vert. emit. ε_y [pm]	1.40	4.32	1.29	2.98
Hor. IP beta β_x^* [mm]	110	200	300	1000
Vert. IP beta β_y^* [mm]	0.7	1.0	1.0	1.6
Lifetime* [min.]	22	17.8	10	12.3

MECHANICAL MODEL OF THE IR

In the IR, the separate beam pipes hosting the two beams are merged together into a single vacuum chamber. The general beam pipe section before and after the merger is circular. An horizontal SR mask is placed after QC1, at 2.12 m from the IP. A circular mask is foreseen between QC2 and QC1, as the physical aperture is reduced from 20 to 15 mm radius. The present geometry of the IR beam pipe differs from the CDR design mainly by the inner radius of the central inner pipe, which now is 10 mm instead of 15 mm, allowing for better resolution in the physics reconstruction. The smaller size of the central pipe also decreases the geometrical impedance and moves the unavoidable trapped mode to a higher frequency. The impedance-related heat-load distribution evaluated through CST wakefield calculations has been fed into ANSYS simulations to develop the beam-pipe cooling system. For the central chamber, the cooling will be based on paraffin flowing inside a double layer structure composed of two concentric cylinders. Outside the innermost part of the central chamber and until the lumical, water cooling is considered, with the help of asymmetric thick copper channels deposited on the AlbeMet162 trapezoidal chamber [10].

We have engineered the very central region of the IR, as shown in Fig. 2. The mechanical design includes the vacuum chamber with the cooling system, the bellows, the vertex and outer tracker detectors, and a carbon-fibre lightweight support structure that will also hold the lumical. This support tube, consisting of an empty cylindrical multilayer rigid structure, eases the integration of the accelerator and detector components, providing a cantilevered support for the central beam pipe. A structural analysis of this design shows good resistance to stress and displacement. Thanks to this support tube we have implemented a preliminary assembly

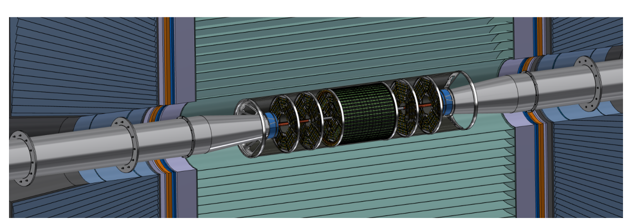

Figure 2: Section of the MDI CAD model for about ±1.5 m around the IP. The beam pipe, the lumical, the vertex and outer trackers, will all be held by the support tube shown here with its endcaps.

ISBN: 978-3-95450-231-8 ISSN: 2673-5490 doi: 10.18429/JACoW-IPAC2023-MOPA091

sequence for this central region. Two bellows on either side of the IP are designed adapting the ESRF design [11] to the small longitudinal space available, about 70 mm. An evolution of the detector IDEA concept has been studied to integrate the silicon tracker in the IR. It features a vertex detector, closer to the beam pipe, made of MAPS detectors, and an outer tracker, at a larger radius, composed of a barrel section and forward disks made of DMAPS silicon pixel detectors. This detector is being implemented in full simulation. A similar study is also planned for the CLD vertex detector. A non-invasive and radiation resistant alignment and monitoring system is being studied to provide the required precision at the level of tens of microns for the MDI components thanks to an external system, based on the Frequency Scanning Interferometry (FSI), and an internal one, based on innovative in-line multiplexed and distributed FSI monitoring portions of fibers placed in helices shape along the supports of the screening and compensating solenoids [12]. We have recently proposed a complementary R&D activity of a full-scale IR mock-up to be realised at Frascati. It will allow us to test technological solutions with prototypes of key components, to verify the vertex detector air cooling system, and to anticipate any possible assembling issue. The IR mock-up will eventually be available for further studies on stability, alignment, and vibrations.

DETECTOR BACKGROUNDS

The main sources of background from SR come from the last dipole magnet before the IP, the solenoid fringe field, and the FFQ. The particle distribution in the non-Gaussian beam tails plays an important role in the latter magnetic elements. The transverse beam tails are difficult to predict and depend on the stored beam conditions. The study is perfomed with BDSIM [13], utilising the GEANT4 [14] toolkit.

The simulation model starts from the last dipoles, and it includes the solenoid and compensating solenoid field map, the IR quadrupoles, a custom central beam pipe in a GDML

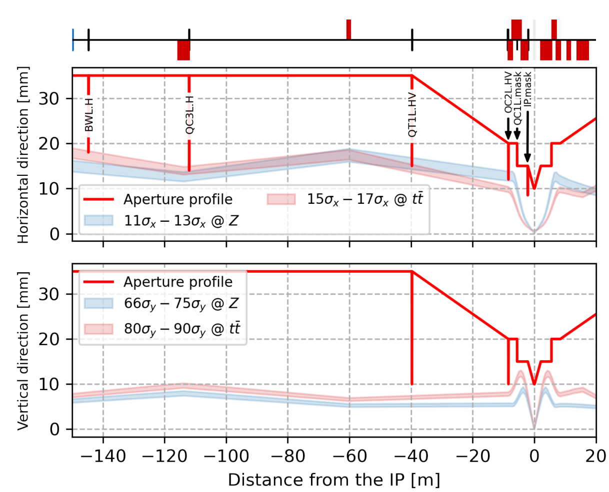

Figure 3: SR horizontal and vertical collimators, and masks.

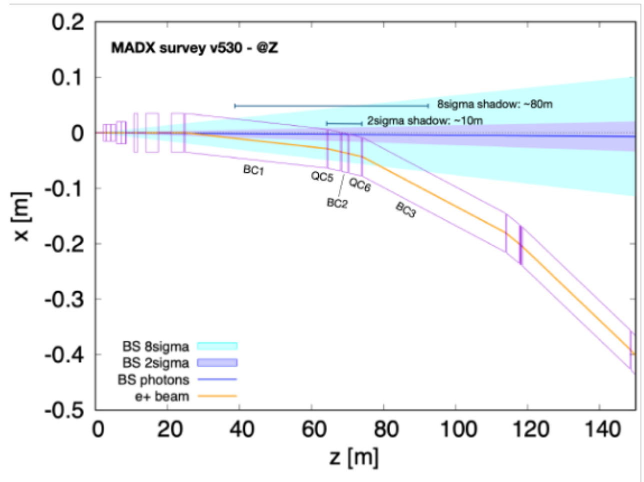

Figure 4: Beamstrahlung photon and electron beam lines, starting from the IP.

format, 10 cm collimators and 2 cm tungsten masks. The MAD-X optics for the four operation modes is converted to input files for BDSIM [15].

Simulations showed that the synchrotron radiation caused by the particles in the beam core from the last dipole magnet onwards reaches the IP whereas the one from the solenoidal field hit mostly 65 m downstream the IP. The SR from the FFQ and solenoid fringe field lead to an increasing power deposition near the IP as the transverse beam tails widen.

SR collimators have been implemented in the IR region to intercept the radiation upstream of the IR. Their positions are shown in Fig. 3. The blue and red filled curves highlight the aperture corresponding to the primary and secondary beam halo collimators for the Z and $t\bar{t}$ operation modes respectively.

The beam halo collimation system has been designed and installed in section PF (see Fig. 1), and has been studied in simulations using the newly-developed Xtrack-BDSIM coupling simulation framework [16]. Good protection has been demonstrated against beam losses due to a beam lifetime drop to 5 min at the most critical Z mode [17].

The MDI description in Key4HEP was implemented with the 10 mm radius central beam pipe and with the solenoidal field map to evaluate the occupancy in the CLD from SR, beam losses and IP backgrounds. Results are encouraging [18], the maximum occupancy per bunch crossing is below the safe 1% level, which is also consistent with the CDR studies [19, 20].

RADIATION FROM THE IR

The radiation produced at the IP is mostly collinear with the exiting beam and hits the vacuum chamber at the first dipole magnet. While this radiation is predominantly due to beamstrahlung, other sources such as radiative Bhabhas and synchrotron radiation are also important. Beamstrahlung radiation from the colliding beams is intense [21] on the order of 400 kW at the Z-pole. This radiation hits the vacuum

ISBN: 978-3-95450-231-8 ISSN: 2673-5490 doi: 10.18429/JACoW-IPAC2023-MOPA091

chamber inside or behind the first bending magnet at about 65 m from the IP. A high-power photon dump is necessary to dispose of this radiation, as well as all the other radiation produced at the IR. Studies performed with GuineaPig++ show that the photon line is separated by the electron beam line by 1 m at about 250 m, and that a dump with a separate alcove and safety shield can be located at about 500 m [22] (see Fig. 4). A preliminary study of a special dipole with a large aperture yoke that can allow the extraction of these photon [23] has been performed.

CONCLUSIONS

We have described recent progress of the FCC-ee MDI study including, a mechanical model of the central interaction region, the mitigation of SR backgrounds, and early studies of local beam losses with a preliminary set of collimators. A first look at the expected detector backgrounds is encouraging. We have also reviewed other MDI-related studies such as the handling of beamstrahlung and the early conceptual design of a photon dump, located downstream of the IR, for this intense radiation.

REFERENCES

[1] A. Abada *et al.*, "FCC-ee: The Lepton Collider: Future Circular Collider Conceptual Design Report Volume 2", *Eur. Phys. J. Spec. Top.*, vol. 228, pp. 261–623, 2019. doi:10.1140/epjst/e2019-900045-4

[2] A. Abada *et al.*, "FCC-hh: The Hadron Collider: Future Circular Collider Conceptual Design Report Volume 3", *Eur. Phys. J. Spec. Top.*, vol. 228, pp. 755–1107, 2019. doi:10.1140/epjst/e2019-900087-0

[3] M. Boscolo, H. Burkhardt, K. Oide, and M. K. Sullivan, "IR challenges and the machine detector interface at FCC-ee", *Eur. Phys. J. Plus*, vol. 136, p. 1068, 2021. doi:10.1140/epjp/s13360-021-02031-5

[4] M. Zobov *et al.*, "Test of crab-waist collisions at DAFNE Phi factory", *Phys. Rev. Lett.*, vol. 104, p. 174801, 2010. doi:10.1103/PhysRevLett.104.174801

[5] K. Oide *et al.*, "Design of beam optics for the Future Circular Collider e^+e^--collider rings", *Phys. Rev. Accel. Beams*, vol. 19, p. 111005, 2016. doi:10.1103/PhysRevAccelBeams.19.111005

[6] M. Dam, "Challenges for FCC-ee luminosity monitor design", *Eur. Phys. J. Plus*, vol. 137. p. 81, 2022. doi:10.1140/epjp/s13360-021-02265-3

[7] K. Oide, "Optics overview", presented at FCCIS workshop, CERN, Dec. 2022

[8] G. Kirby *et al.*, *J. Phys. Conf. Ser.*, vol. 1559, p. 012070, 2020. doi:10.1088/1742-6596/1559/1/012070

[9] B. Parker, "Correctors and Anti-solenoids Design for FCC-ee, MDI Workshop", CERN, Oct. 2022, https://indico.cern.ch/event/1186798/.

[10] A. Novokhatski, M. Boscolo, F. Fransesini, and S. Lauciani, "Estimated heat load and proposed cooling system in the FCC-ee IR beam pipe", presented at IPAC'23, Venice, Italy, May 2023, paper MOPA092, this conference.

[11] Th. Brochard, L. Goirand, and J. Pasquaud, "Dispositif de raccordement entre tronçons d'anneau de synchrotron", B14959 EP, request number 17160419.2 -1211 / 3223591 claiming priority of patent FR 16/52454, Mar. 22, 2016.

[12] L. Watrelot *et al.*, "Frequency scanning interferometry based deformation monitoring system for the alignment of the FCC-ee machine detector interface", *Meas. Sci. Technol.*, to be published. doi:10.1088/1361-6501/acc6e3

[13] L. J. Nevay *et al.*, "BDSIM: An Accelerator Tracking Code with Particle-Matter Interactions", *Comput. Phys. Commun.*, vol. 252, p. 107200, 2020.

[14] J. Allison, *et al.* "Recent developments in Geant4", *Nucl. Instrum. Meth. A*, vol. 835, pp. 186–225, 2016. doi:10.1016/j.nima.2016.06.125

[15] K. D. J. André, 6th FCC Physics workshop, Krakow (Poland), Jan. 2023. https://indico.cern.ch/event/1176398

[16] A. Abramov *et al.*, "Development of Collimation Simulations for the FCC-ee", in *Proc. IPAC'22*, Bangkok, Thailand, Jun. 2022, pp. 1718–1721. doi:10.18429/JACoW-IPAC2022-WEPOST016

[17] A. Abramov *et al.*, "Studies of Layout and Cleaning Performance for the FCC-ee Collimation System", presented at IPAC'23, Venice, Italy, May 2023, paper MOPA128, this conference.

[18] A. Ciarma, M. Boscolo, G. Ganis, and E. Perez, "Machine Induced Backgrounds in the FCC-ee MDI Region and Beamstrahlung Radiation", in *Proc. eeFACT'2022*, Frascati, Italy, Sep. 2022, pp. 85–90. doi:10.18429/JACoW-eeFACT2022-TUZAT0203

[19] G. Voutsinas *et al.*, "FCC-ee interaction region backgrounds", *Int. J. Mod. Phys. A*, vol. 35, p. 2041009, 2020. doi:10.1142/S0217751X20410092

[20] M. Boscolo *et al.*, "Machine Detector Interface for the e+e- Future Circular Collider", in *Proc. eeFACT'18*, Hong Kong, China, Sep. 2018, pp. 201. doi:10.18429/JACoW-eeFACT2018-WEXBA02

[21] M. Boscolo *et al.*, "Challenges for the Interaction Region Design of the Future Circular Collider FCC-ee", in *Proc. IPAC'21*, Campinas, Brazil, May 2021, pp. 2668–2671. doi:10.18429/JACoW-IPAC2021-WEPAB029

[22] F. Valchkova-Georgieva, "Tunnel Integration", presented at FCCIS 2022 Workshop, https://indico.cern.ch/event/1203316/.

[23] C. J. Eriksson and J. Bauche, "Magnet Design for Beamstrahlung Photons Extraction Line", presented at FCC-ee MDI meeting, Feb. 2023.